



U-shape functionalized optical fibre sensors for measurement of anaesthetic propofol

Francisco U. Hernandez^{a,b,*}, T. Wang^b, Seung-Woo Lee^{b,**}, A. Norris^c, LiangLiang Liu^a, B. R. Hayes-Gill^a, S.P. Morgan^a, S. Korposh^{a,*}

^a Optics and Photonics Group, Faculty of Engineering, University of Nottingham, Nottingham NG7 2RD, UK

^b Department of Chemical and Environmental Engineering, University of Kitakyushu, 1-1 Hibikino, Kitakyushu, Fukuoka 808-0135, Japan

^c Department of Anaesthesiology, King Faisal Specialist Hospital and Research Centre, Riyadh, Saudi Arabia

ARTICLE INFO

Keywords:

Optical fibre sensors (OFS)
U-shaped fibre
Propofol
Host-guest
Cyclodextrins
Titanium dioxide (TiO₂)

ABSTRACT

Propofol is used widely for intravenous anaesthesia during surgery and sedation in critical care. There is no method currently to assay the concentration of propofol in plasma in real time. The ability to do so would significantly improve patient safety. A novel approach to propofol assay consisting of Beta-Cyclodextrin (β - CD) assisted propofol-imprinting onto TiO₂ films deposited on U-shaped optical fibres was used for the measurement of propofol in aqueous solutions. The sensing mechanism is based on the measurement of the refractive index change induced by the removing and binding of the propofol from and to the β - CD/propofol complex embedded onto TiO₂ films, respectively. Complexation between host (β - CD) and guest (propofol) was confirmed by nuclear magnetic resonance (NMR) spectroscopy, UV-Vis spectroscopy, and by Attenuated Total Reflectance- Fourier-transform infrared spectroscopy (FTIR). The developed sensors presented Langmuir adsorption in the mM range and the lowest concentration detected was 0.69 μ M= 0.12 μ g/ml. The approach can be replicated for other compounds in other biomedical applications such as vitamins, hormones, or drugs.

1. Introduction

Continuous total intravenous infusion (TIVA) of propofol is the main method of maintaining general anaesthesia in approximately 25% of surgical procedures [1]. It has advantages over the alternative, namely, use of inhaled agents. Advantages of TIVA include improved recovery and reduced environmental impact [2,3]. However, TIVA has one major limitation over inhalation techniques: there is no current method to measure propofol concentration in the blood during surgery. In contrast, inhaled vapour monitoring has been available for over 30 years, initially by mass spectrometry, and now infrared absorption.

Knowledge of anaesthetic agent concentration is critical to maintenance of an appropriate depth of anaesthesia, provides strong reassurance that appropriate doses are reaching the patient, and allows titration administration rate against a measurable end point. In the absence of ability to measure concentration in the patient, TIVA must instead rely on pharmacokinetic modelling of drug behaviour, clinical signs in the patient, and increasingly, monitoring of both electroencephalogram

(EEG) and electromyography activity to improve clinical utility of monitoring [4]. All these methods have significant technical complexity and labour-intensive methodology, which include proper functioning, set up, programming and use of all delivery equipment such as infusion pumps and intravenous lines, accurate and advanced pharmacokinetic modelling for target-controlled infusion, the presence of typical arousal signs in unconscious subjects, and processed brain activity that looks backwards in time with no predictive value and reliable reaction to stimulus [5]. The ability to reliably measure blood or breath propofol concentration in real time in the operating room or intensive care unit would therefore represent a breakthrough in anaesthesia safety.

The desired clinical concentration of propofol in plasma ranges from 1 to 10 μ g/ml [6] and several attempts have been made to measure propofol concentration in this range. Potential measurement methods including High-Performance Liquid Chromatography (HPLC) [7] and Gas Chromatography-Mass Spectrometry [8] have been investigated, but all have limitations such as long response time, time-consuming for sample preparation, and the devices are bulky and expensive.

* Correspondence to: Faculty of Engineering, The University of Nottingham, University Park, Nottingham NG7 2RD, UK.

** Corresponding author.

E-mail addresses: francisco.hernandez@nottingham.ac.uk (F.U. Hernandez), leesw@kitakyu-u.ac.jp (S.-W. Lee), s.korposh@nottingham.ac.uk (S. Korposh).

<https://doi.org/10.1016/j.snb.2022.132653>

Received 1 April 2022; Received in revised form 8 September 2022; Accepted 9 September 2022

Available online 13 September 2022

0925-4005/© 2022 The Authors. Published by Elsevier B.V. This is an open access article under the CC BY license (<http://creativecommons.org/licenses/by/4.0/>).

Monitoring of propofol by optical fibres has been proposed in two research studies: (i) Li and Li [9] proposed a rapid measurement (10 min to ensure steady state) of propofol in plasma samples by the implementation of an optical fibre based spectrophotometric system containing a broadband light source and a spectrometer to measure absorbance through a Z-flow cell. This cell was connected to a sequential injection system that mixed propofol with diazonium salt (azo-coupling reaction). A limit of detection (LoD) of 0.65 $\mu\text{g/ml}$ was reported, and results were compared with UV-Vis spectroscopy. (ii) Li et al. [10] validated against HPLC, a method utilizing on-line molecularly imprinted polymer solid-phase extraction (SPE) coupled to fluorescence optical fibre detection. The set-up proposed in this study used optical filters and collimators, it was based on fluorescence measurements after reaction of propofol with Gibb's reagent (5 min to complete entire analysis) and demonstrated a detection range in simulated whole blood samples between 0.10 and 15 $\mu\text{g/ml}$.

In other relevant research, Hong et al. [6] built a lab-on-chip system using micro-optical components and a disposable microfluidic biochip (molecularly imprinted). The total size of the system was 448 cm^3 and dynamic measurement of propofol was reported after reaction with colour reagent (Gibbs and bicarbonate buffer). All measurements were achieved within 90 s and this technique reached a LoD of 0.25 ppm (1.4 μM) within a range between 0.25 and 10 ppm for in vitro solutions of propofol in methanol solvent. McGaughan et al. [11] demonstrated propofol measurement from blood of 17 patients using SPE coupled with colorimetric and spectrometric techniques (validated with HPLC). The study reported absorbance measurements within an approximate range of detection of 0.5 – 10 $\mu\text{g/ml}$ and a run time of 4.5 min per sample (including preparation). Liu et al. [12] validated against HPLC, a medical device (Pelorus 1000, Sphere Medical, UK) also based on colorimetric techniques, SPE and coupled with absorbance spectroscopy. This study reported a LoD of 0.27 $\mu\text{g/ml}$ in whole blood and a run time of 5 min without the requirement for sample preparation.

The common characteristic of all the previous methods was an analysis and response time close to real time (minimum 4.5 min). Only Kivlehan et al. [13] proposed a different portable device for the same purpose, consisting of a membrane-coated electrochemical sensor embedded onto the surface of an intravenous catheter to test concentrations of propofol samples with faster reading response of 10 s. The electrochemical sensor containing a membrane coated with polyvinyl chloride was validated against HPLC and demonstrated a LoD of 0.08 \pm 0.05 μM in aqueous solutions and a LoD of 1.25 μM when measures were taken with propofol spiked in whole blood samples. More recently, Stradolini et al. [14] built a propofol monitoring system which also uses electrochemical cells with pencil graphite electrodes (graphite, clay and wax) for fouling-free detection and without interference compounds (LoD of 0.53 μM \pm 0.03% of relative standard deviation).

The chemical sensing method proposed in this research is based on the molecular imprinting of binding sites of propofol using the host-guest interaction between cyclodextrin-propofol and imprinted onto titanium dioxide (TiO_2) films using the Liquid Phase Deposition (LPD) technique. This method was previously demonstrated by our research group [15] by utilizing Long Period Grating (LPG) fibre sensors as the functionalized transducer platform but this is the first time this has been demonstrated on a U-shaped optical fibre sensor (OFS). Although other configurations of optical fibre sensor such as tapered or interferometric are available that may provide higher sensitivity in biomedical applications [16] or industrial applications [17], a U-shaped configuration is preferred as it provides a simple implementation with a sensitive and robust platform for sensing purposes. This work extends the full characterisation of this molecular imprinting approach (aided using cyclodextrins) with the help of spectroscopic techniques and with the deposition of the sensing film onto a U-shaped OFS as the transducer platform for the measurement of propofol in aqueous solutions. The main difference between the previous optical techniques [9–12] and the approach of this research consists mainly in the method of measuring the

propagation of light and its interaction with the sample exposed to propofol solutions. Previous approaches [9–12] use conventional UV-Vis spectroscopy, i.e., the absorbance or fluorescence of samples (molecularly imprinted or solid-phase extracted) is measured by shining light on one side and collecting (with fibres or micro-optical components) the light scattered or transmitted through the sample on the other side. The approach used in this work detects capture of propofol on the surface of the U-shaped optical fibre with the aid of cyclodextrins. Cyclodextrins (Fig. 1a) are biocompatible and have been used as a host compounds for other type of analytes such as amino acids and polypeptides, oligonucleotides as therapeutic agents, serum lipoproteins, and to facilitate dissolution of low solubility compounds in tissue and cell culture involving drug delivery [18–21]. Measurement of propofol (Fig. 1b) in this research was feasible through the host-guest interaction between cyclodextrin-assisted propofol binding sites embedded in TiO_2 films created at the surface of the optical fibres thus opening an opportunity for in vivo measurements.

2. Materials and methods

2.1. Materials

Propofol (2,6-Diisopropylphenol, $M_w=178.3$ g/mol), Ethanol (99%), Sodium Hydroxide (NaOH, $M_w=40$ g/mol) and Potassium Hydroxide (KOH, ACS reagent, pellets) were bought from Sigma Aldrich. Beta-Cyclodextrin (β -CD, $M_w=1134.98$ g/mol) from Tokyo Chemical Industry Co. Ltd; Ammonium Hexafluorotitanate $[(\text{NH}_4)_2\text{TiF}_6]$ ($M_w=197.93$ g/mol) from Mitsuwa Chemical Co. Ltd; Boric Acid (H_3BO_3 , $M_w=61.83$ g/mol) from Wako Pure Chemical Industries Ltd; deionized water (resistivity 18.2 Megaohm \cdot cm) was obtained by reverse osmosis and subsequently subjected to ion exchange and filtration in a Milli-Q apparatus.

2.2. Host-guest complexation study with nuclear magnetic resonance (NMR) spectroscopy

Proton ^1H NMR spectroscopy level [22] was used to demonstrate the inclusion between β -CD (host) and propofol (guest molecule) using a 500 MHz FT NMR (JEOL USA Inc.). The solvent used to dissolve these host-guest molecules was 10% (v/v) deuterated dimethyl sulfoxide ($\text{DMSO-}d_6$) in deuterium oxide (D_2O). Solutions with β – CD : Propofol complexes of ratios (1:1), (2:1) and (3:1) were prepared in the same solvent ($\text{DMSO-}d_6$: D_2O) and analysed through ^1H NMR spectroscopy when compared to pure solution of β – CD (10 mM) in the same solvent. Similarly, the same complexation ratios of solutions (β – CD : Propofol) were compared with the pure solution of propofol (10 mM) measured separately under the same solvent.

2.3. U-shaped (probe): fabrication and sensing principle of operation

To fabricate U-shaped probes, first the plastic jacket is removed from the optical fibre with a stripping tool (T12S21, Thorlabs Inc) and then the buffer coating and cladding of the fibre are reduced while simultaneously exposing to a propane flame and deforming it into a U-shape until the desired bending radius is reached. The sensing principle of a U-shape fibre probe is based on the fraction of the power from the evanescent wave at the core-cladding interface, and the bending of the fibre shifts the propagation modes away from the centre of curvature to interact with the analytes present in the surrounding medium [23,24]. There are two theoretical methods to explain the sensing principle of the U-shaped probe: (1) The beam propagation method (BPM) in combination with conformal mapping allows to obtain the propagation modes and predict bend loss against bend radius of both single-mode and multimode fibres [24]; (2) ray theory approximations can be used to calculate penetration depth of the evanescent wave generated in the sensing region when light is launched into the fibre (Fig. 2). The

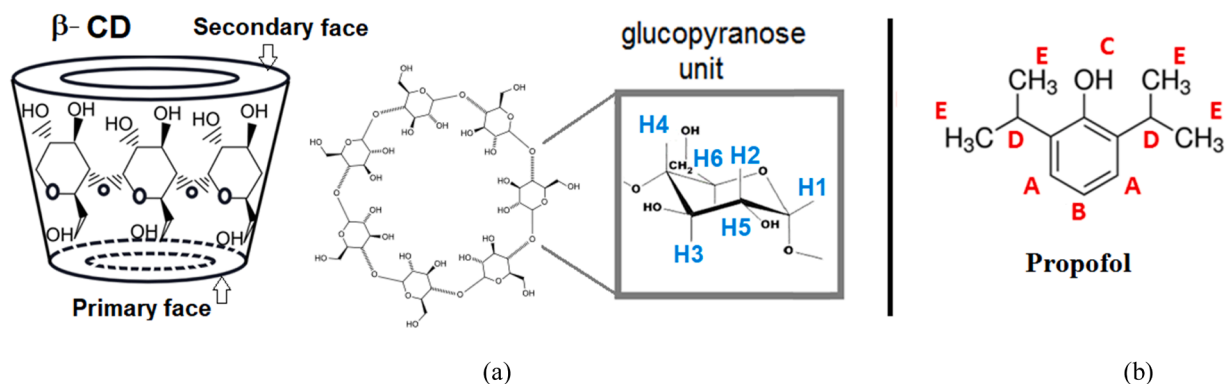


Fig. 1. (a) Beta Cyclodextrins (hosts) and (b) propofol molecule (guest) can form inclusion complexes through host-guest interactions. The protons (magnetic isotopes of hydrogens) of the cyclodextrins are shown in blue in (a) and the protons of propofol are shown in red in (b). The interaction of these protons is demonstrated through Nuclear Magnetic Resonance (NMR) spectroscopy.

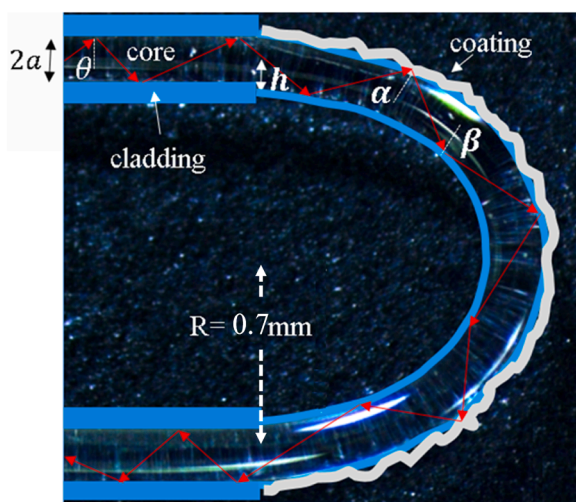


Fig. 2. Photograph of a fabricated U-shaped fibre (radius $R=0.7$ mm) having a schematic illustration of the cladding, a nano-thin film coating and the light rays propagating inside the core (radius $a=100$ μm). The parameter θ is the angle of incidence with respect to the normal to the core-cladding interface, h is the ray's entrance height, β is the angle of the ray in the inner bent region and α is the angle of the ray in the outer bent region with the normal to fibre-film interface.

appearance of lossy resonance modes can be demonstrated when the outer surface of U-shaped probes are coated with a thin film material having higher refractive index than the reduced cladding (sensing region) [25,26]. In regard to the coupling of light at the interface between cladding, the imprinted TiO_2 film and the surrounding medium, Kaur et al. [26] have published the mathematical approach to explain the design of waveguide sensors to support guided modes or lossy resonance modes when there is a structure configuration of silica / material with higher refractive index (e.g. TiO_2) / dielectric layer ($n_{\text{water}} = 1.33$). A similar approach has been investigated by Paliwal et al. [25] for the case of U-shaped sensors coated with ZnO to create lossy resonance modes. These two publications describe the mathematical foundations for the enhancement of the evanescent field and the sensitivity of the sensors based on various parameters such as the resonance and incidence angles, film thickness and the effective refractive index of the coating layer.

Recently, Danny et al. [27] demonstrated a model based on ray optics for describing the main parameters affecting the U-bent plastic optical fibre (POF) sensors' sensitivity to refractive index change. In summary, the refractive loss and sensitivity at the bend region were demonstrated to be highest when the bend ratio (Bending radius/core

radius, R/a in Fig. 2) was smaller than 7 when the inhomogeneity effects are considered due to bending/deformation of the core of the fibre. The model predicts that the sensitivity starts to increase for $R/a < 15$ (saturation regime) and the selection of $R = 0.7$ mm, $a = 100$ μm ensures the fabricated sensor lies within the regime with highest sensitivity. Although Danny et al. [27] demonstrated the effect of inhomogeneity in the material properties due to bending/deformation of the core (elasto-optic coefficients and Poisson's ratio) in POFs, the model can be extended to optical fibres with silica core (multimode fibre with Technology Enhanced Clad Silica -TECS- hard polymer cladding, FT200 EMT Thorlabs Inc) [28].

2.4. Liquid-phase deposition (LPD) for imprinted or non-imprinted TiO_2 films

In this investigation, the LPD process (Section 1 of Supplementary Material) was used to deposit TiO_2 on the surface of all the three: glass substrates, gold-coated silicon wafer substrates and U-shaped optical fibres (Fig. 3). The application of the LPD process was implemented onto glass or gold-coated silicon wafer substrates to support the characterization and differentiation of imprinted and non-imprinted TiO_2 films with the help of spectroscopic techniques such as UV-Vis spectroscopy (using glass substrates) and Fourier Transform Infrared (FTIR) spectroscopy (using gold-coated silicon wafer substrates). The U-shaped fibre section used for every LPD functionalization was ca. 2 cm and the total length of every fibre was ca. 150 cm.

The LPD process followed the procedure:

- (i) *Preparation of stock solutions* - β - CD:Propofol (1:1) complex was prepared as an aqueous stock solution with the concentration of 1.6 mM which was sonicated and then stirred for more than 3 h at c.a. 30 $^\circ\text{C}$; there were two sets of concentrations for the stock aqueous solutions of $[\text{NH}_4]_2\text{TiF}_6$ and H_3BO_3 . Set 1 was based on 100 mM of $[\text{NH}_4]_2\text{TiF}_6$ and 200 mM of H_3BO_3 . Set 2 was based on 200 mM of $[\text{NH}_4]_2\text{TiF}_6$ and 400 mM of H_3BO_3 .
- (ii) *Hydroxylation of substrate or U-shaped optical fibre surface* - glass substrates or the U-shaped probe were immersed in 1 wt% of ethanolic KOH (ethanol/water = 3:2, v/v) solution for 20 min and using the set-up shown in Fig. 3.
- (iii) *Mix and functionalization of substrate or U-shaped optical fibre surface* (Fig. 3) - After hydroxylation, washing with deionised water and drying with nitrogen, either the substrate (Fig. 3a) or the U-shaped probe (Fig. 3b) were immersed in either Set 1 or Set 2 of concentrations. Set 1 consisted in mixing the precursor solutions as follows: 1 ml of complex β - CD:Propofol, 0.5 ml of (100 mM $[\text{NH}_4]_2\text{TiF}_6$) and 0.5 ml of (200 mM H_3BO_3) to obtain the final concentrations of 0.8 mM β - CD:Propofol, 25 mM

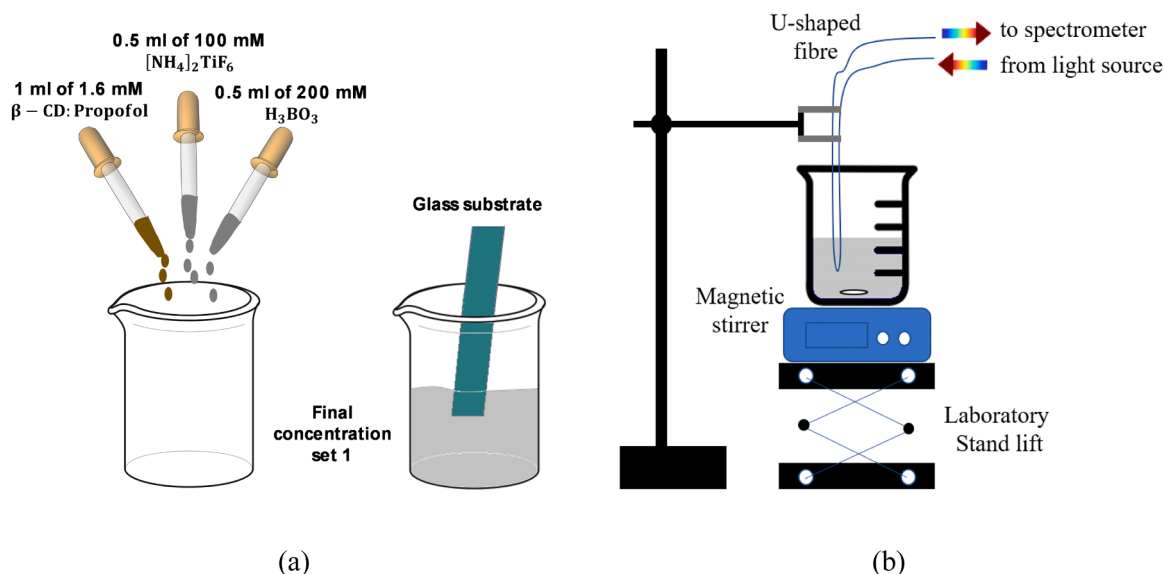


Fig. 3. (a) Example of the method for implementing the LPD process to obtain imprinted (with β -CD:Propofol) TiO_2 films onto glass substrates. (b) Set-up for functionalizing U-shaped fibres; a magnetic stirrer is advisable during the LPD process and during continuous test for measurement of propofol.

$[\text{NH}_4]_2\text{TiF}_6$ and 50 mM H_3BO_3 . Set 2 consisted of mixing 1 ml of complex β -CD:Propofol, 0.5 ml of (200 mM $[\text{NH}_4]_2\text{TiF}_6$) and 0.5 ml of (400 mM H_3BO_3) to obtain the final concentrations of 0.8 mM β -CD:Propofol, 50 mM $[\text{NH}_4]_2\text{TiF}_6$ and 100 mM H_3BO_3 . The mixture either with Set 1 or Set 2 was stirred until all the compounds were mixed uniformly (few seconds) and used as the solution for the imprinted functionalization on substrates or U-shaped optical fibres (as shown in Fig. 3). In parallel, non-imprinted TiO_2 (only $[\text{NH}_4]_2\text{TiF}_6$ and H_3BO_3) films were also prepared under the same environmental conditions and concentrations (25:50 mM or 50:100 mM) for the purpose of comparison in the characterization of these films and their performance for the measurement of propofol.

- (iv) *Deposition time for the LPD process with imprinted and non-imprinted TiO_2 films onto substrates or optical fibres (Fig. 3)* - Our previous research has demonstrated a suitable functionalization time between 14 and 18 h with LPG sensors [15]. The sensitivity to evanescent wave performance (or lossy mode resonance) also depends on film thickness, therefore, this research tested functionalization times between 12 and 21 h (room temperature of 24 °C) for U-shaped fibres. The case of gold-coated silicon wafer substrates and glass substrates considered a film deposition time of 21 h and 26 h respectively to increase the detection sensitivity, by providing larger number of binding sites, of the spectroscopic devices used (FTIR and UV-Vis spectroscopy). Only one U-shaped fibre was functionalized for 41 h to support evidence of the sensing principle and demonstrate that the increase of film thickness has an impact on the light propagation (losses) in the U-shaped optical fibre.
- (v) *Template removal* - The template (propofol) needs to be removed (washed out) from the β -CD:Propofol binding sites generated within the imprinted TiO_2 film. This was achieved by washing the fibre or substrate surface (the imprinted TiO_2 film case) with ethanol for 5 min at room temperature.

Fig. 3a shows the set-up used for the deposition of the imprinted TiO_2 on glass substrates (after hydroxylation) and add the Set 1 of concentrations for functionalization. On the other hand, the set-up shown in Fig. 3b keeps fixed the U-shaped probes which are immersed in the beakers containing the prepared deposition solutions (imprinted or non-imprinted). One arm of the U-shaped fibre was connected to a

spectrometer (HR-2000, Ocean Optics) and the other to a tungsten-halogen lamp (HL-2000, Ocean Optics). Data from the spectrometer was recorded in a PC using the OOIBase32 operating software also from Ocean Optics; this software allows recording of the spectra of transmitted light and the intensity of specific wavelengths by tracking every 5 ms.

The set-up of Fig. 3b allowed interchange of different beakers containing the prepared solutions, for instance, the sequence for implementing the LPD process onto U-shape probes followed the next steps:

- (i) Immersion of fibre in beaker containing 1 wt% of ethanolic KOH for 20 min
- (ii) Immersion of fibre in a different beaker containing any solution with either Set 1 or Set 2 concentration (with β -CD:Propofol for the imprinted case and without complex for the non-imprinted case). Depending on the concentrations used, the formation of the imprinted TiO_2 film onto the surfaces started to be visible after 10 h of immersion/deposition.
- (iii) The last immersion of the fibre was in a beaker with ethanol for 5 min. This was done with the purpose of removing/washing the template from the imprinted TiO_2 film and having a ready imprinted sensor for measurement of the target propofol.

2.5. Fourier transform infrared (FTIR) spectroscopy

An FTIR spectrometer (Spectrum 100, Perkin Elmer) coupled with an Attenuated Total Reflectance (ATR) accessory were used for characterizing the differences between imprinted TiO_2 and non-imprinted TiO_2 films. In this method, gold-coated silicon wafer substrates were cleaned (ethanol and deionized water), dried with N_2 and surface activated with plasma treatment (Covance used at 0.24 torr of vacuum, FemtoScience) for further thin film deposition using the LPD process described in Fig. 3a. Thus, after plasma activation, the substrates were coated using the LPD process with the concentrations of Set 1 and a deposition time of 21 h for the imprinted TiO_2 case on the one hand, and the same final concentrations of $[\text{NH}_4]_2\text{TiF}_6$: H_3BO_3 (25 mM: 50 mM) on the other for creating a non-imprinted TiO_2 film onto the gold coated substrate. In both cases, imprinted and non-imprinted films, the upper limit of the optimal deposition time (21 h) was chosen to functionalize the substrates to increase the detection sensitivity of the spectrophotometer. After imprinting and non-imprinting TiO_2 LPD deposition onto the gold

coated substrates, these were tested in the ATR-FTIR spectrophotometer. The FTIR spectrum from a gold coated substrate was taken as a reference baseline for the subsequent acquisition spectra of both imprinted-TiO₂ and non-imprinted-TiO₂ films.

2.6. Ultraviolet-visible (UV-Vis) spectroscopy

This technique was applied as a complementary method to ATR-FTIR for further characterizing the differences between imprinted and non-imprinted TiO₂ films. An UV-Vis spectrophotometer (V-570 JASCO) was used to confirm the specific absorbance wavelengths of the organic materials hosted onto the TiO₂-based films. In this method, Cyclic Olefin Copolymer (COC) glass substrates were cleaned (ethanol and deionized water), dried with N₂, hydroxylated for 20 min, and further functionalized with the concentrations of Set 1 for 26 h. Another cleaned and dried COC substrate was used as a reference for blank measurements in the UV-Vis spectrophotometer and both imprinted (β -CD:Propofol) and non-imprinted (only [NH₄]₂TiF₆: H₃BO₃) substrates were functionalized as depicted in Fig. 3a with deposition times of 26 h each. Similar to FTIR, a longer deposition time than the upper limit required with fibres was implemented to increase the spectrum acquisition's sensitivity of the UV-Vis spectrophotometer. After functionalization with the LPD process, the imprinted and non-imprinted absorbance spectra were obtained after baseline correction from the blank measurement. Analysis through the second derivative of the UV-Vis spectra was applied as described in [29] and [30] to quantitatively confirm maximum absorption of mixed compounds in a multicomponent system.

2.7. Measurement of propofol in aqueous solutions

For the case of testing the continuous measurement of propofol, the set-up shown in Fig. 3b was implemented while the functionalized U-shaped sensor was immersed in deionised water and under continuous magnetic stirring. Measurement of propofol in the millimolar range was performed using an initial volume of 20 ml of deionised water and using a stock solution of 0.5 mM of propofol which was in turn emptied in a dropwise fashion (using micro-pipettes). Measurement of propofol in the micromolar range was performed using an initial volume of 4 ml of deionised water and using a stock solution of 20 μ M of propofol which was also added dropwise using micro-pipettes. After a stabilization time interval between 3 and 5 min, each concentration of propofol was emptied in the set-up shown in Fig. 3b to evaluate the response of every U-shaped sensor under test.

3. Results

3.1. Host-guest interaction between β -CD and propofol with NMR spectroscopy

One approach to study the host-guest inclusion between β -CD and propofol is through the analysis of the deviation in the chemical shifts of the protons (isotopes of hydrogen shown in Fig. 1) that are used for devising the chemistry reactions of interest when they are mixed and compared in the same solvent (refer to Figs. S1 and S2 of Supplementary Material). A chemical shift is a frequency shift expressed as parts per million (ppm) and measured from a reference resonance frequency of a nucleus [22]. Changes in the chemical shifts of protons indicates variations in the chemical environment of the nuclei from both host and guest molecules and variations similar or greater than 0.05 ppm are considered the most significant in ¹H NMR spectroscopy [31,32]. Section 2 of Supplementary Material provides the raw NMR spectra data of the different complex ratios of β -CD: Propofol when compared with the pure solutions of these molecules. Thus, only the aromatic proton B of the propofol molecules presented significant variations in chemical shift after complexation with β -CD at three different concentrations (Fig. 4a). Similarly, the protons H3 and H5 which are located inside the

conical cavity (Fig. 4b) of the host molecules β -CD, resulted in the most significant changes in chemical shift after complexation at the three different concentration ratios.

3.2. Characterization of imprinted and non-imprinted TiO₂ using ATR-FTIR

Fig. 5 presents the main vibrational modes and wavenumbers associated with TiO₂ and β -CD adsorbed to TiO₂ respectively when measured through FTIR. The National Institute of Standards and Technology (NIST) reports the wavenumbers from the strongest vibrational modes of propofol measured through FTIR which are: 3610 cm⁻¹, 2930 – 2850 cm⁻¹, 1410 cm⁻¹ and 1170 cm⁻¹ [33]. For clarity, Fig. 5 is divided into four sections with vertical dashed lines in order to show the four main vibrational and stretching bands for pure TiO₂ films (non-imprinted) [34] and also for identifying more easily the vibrational and stretching bands for the imprinted TiO₂ case [35–37].

As can be confirmed in Fig. 5, adsorption of the complex β -CD: propofol onto the TiO₂ surface is observed in the appearance of the conformation stretching modes in the range between 1110 and 1160 cm⁻¹, i.e., ν (C – O – C): 1030 cm⁻¹ and ν (C – O): 1158 cm⁻¹. Adsorption is also observed when O – H and N – H bending vibrations: 1400 – 1750 cm⁻¹ are masked with mainly hydroxyl groups (ca 0.1650 cm⁻¹) from the organic complex covering the TiO₂ surface. In addition, adsorption of the organic complex β -CD:Propofol is evidenced through the shift obtained for vibrational modes ascribed to the O – H vibration of water adsorbed onto both films, non-imprinted and imprinted TiO₂ at 3410 cm⁻¹ and 3360 cm⁻¹ respectively.

3.3. Characterization of imprinted and non-imprinted TiO₂ using UV-Vis spectroscopy

Fig. 6a shows the UV-Vis absorption spectrum of the non-imprinted TiO₂ film and imprinted (β -CD:Propofol) TiO₂ film. Fig. 6b presents the second derivative of the UV-Vis spectra. This derivative method [41] is regularly used to quantitatively confirm maximum absorption measurements for compounds mixed in a multicomponent system [29] as the imprinted case in this work.

The result presented in the original absorption spectra (Fig. 6a) confirms the range of absorption for cyclodextrins and propofol in the mid-ultraviolet region between 200 and 300 nm [36]. The second derivative method (Fig. 6b) helps to identify critical points such as the turning point at ca. 286 nm in the original β -CD:Propofol/TiO₂ spectrum (Fig. 6a) which appears as a peak at the same wavelength in Fig. 6b. The maximum absorbance at ca. 326 nm in the original β -CD: Propofol/TiO₂ spectrum (Fig. 6a) results as a negative peak in its second derivative plot (Fig. 6b). Additionally, zero-crossing wavelengths are useful to discriminate between chemical compounds in the overlapping bands [29,42] and the results of Fig. 6b confirm that zero-crossing points are different between the black and red curves. For instance, there are zero-crossing points at wavelengths of 258 nm, 304 nm (with negative peaks for the black curve) and 357.5 nm for the red curve. The wavelength of 286 nm is attributable to the absorbance of propofol [41] and 260 nm as the maximum absorbance of β -CD [36,43,44], however, the absorbance of host-guest molecules tend to be shifted to values higher than 300 nm for guest molecules already hosted by β -CD [29,36,43, 44] which is clearly visible in the imprinted TiO₂ spectra of Fig. 6a and b.

3.4. U-shaped sensor fabrication, functionalization, and measurement of propofol

Table 1 shows the bending radii fabricated, the set of concentrations used for the LPD process and the deposition time for functionalization for each of the U-shaped fibres tested. The desired bending radius was constrained by the manual fabrication set-up and radii between

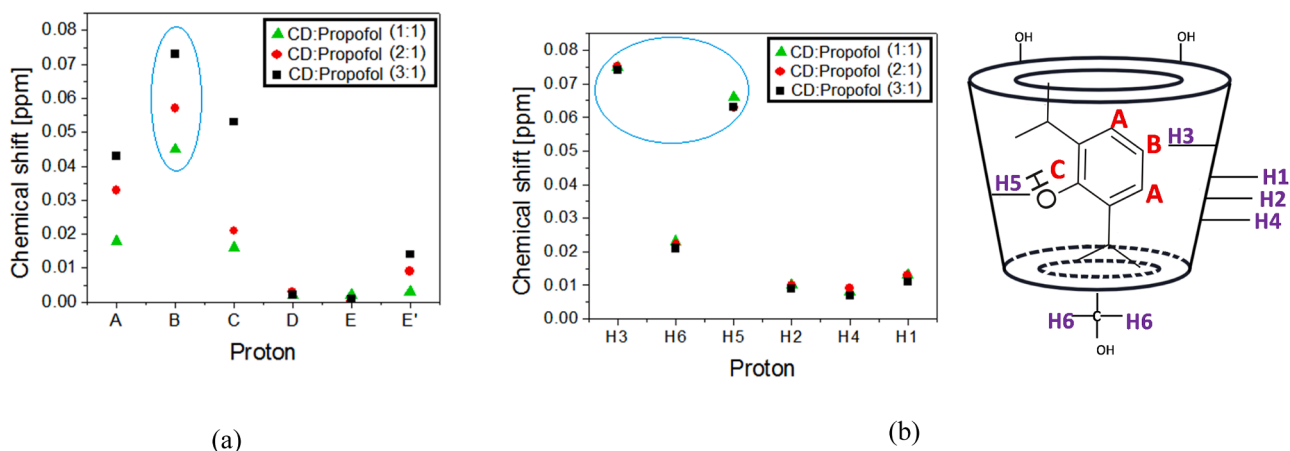


Fig. 4. Summary of the changes in chemical shifts calculated from raw NMR spectrometer data (Section 2 Supplementary Material). (a) Variations for the protons of propofol and (b) variations for the protons of β - CD and representative schematic of the host-guest inclusion demonstrated by the NMR results.

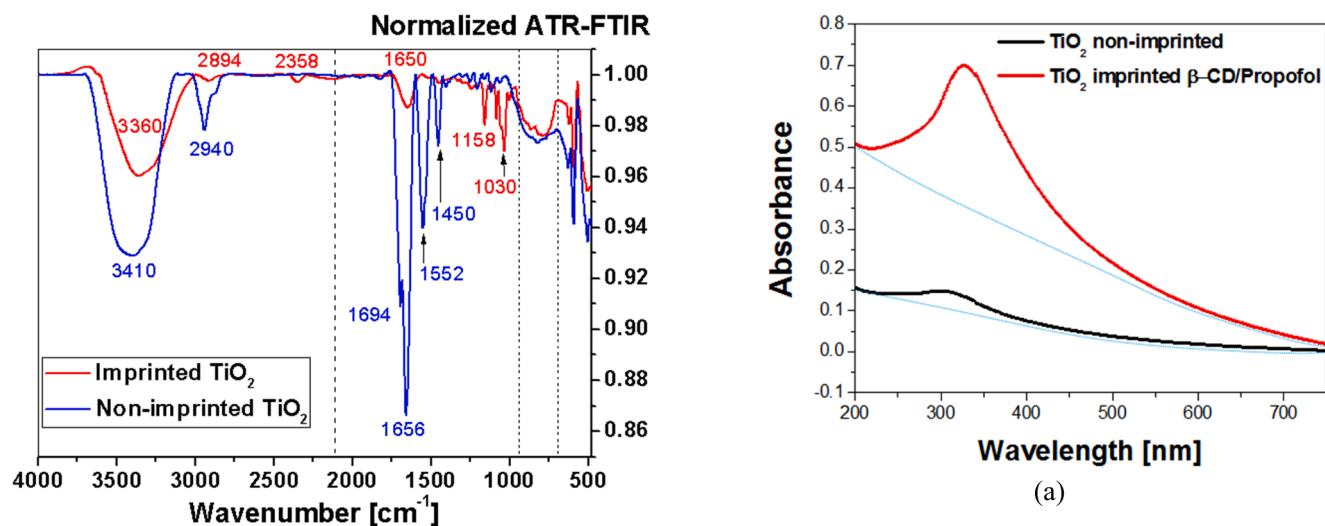


Fig. 5. Comparison of ATR-FTIR spectra between non-imprinted TiO_2 and imprinted TiO_2 . These results can be corroborated with previous research [38–40].

0.65 mm and 0.85 mm were obtained in the U-shaped sensors tested. Before functionalizing, the sensitivity to refractive index change of the U-shaped sensors was measured (Table 1) using different concentrations of ethanol (from 0% to 70% or 90%) in deionised water [45] and implementing the same set-up shown in Fig. 3b in order to normalise the response of different sensors to propofol. Figs. S3 – S9 of Supplementary Material present the refractive index sensitivities of every U-shaped sensor of Table 1.

Fig. 7a presents the transmission spectrum of U1 (Table 1) before and after functionalization through LPD process after 41 h of deposition. Despite an optimal deposition time of $16 \text{ h} \pm 2 \text{ h}$ found in our previous research work with LPGs [15], this research tested longer deposition times to confirm the effects of film thickness growth and respective decrease of power transmission spectra recorded during the LPD deposition. Fig. 7b demonstrates the dynamic evolution of $\lambda = 611 \text{ nm}$ from the transmission spectrum shown in Fig. 7a and during the deposition of the imprinted TiO_2 film. The inset in Fig. 7b shows the signal change due to the hydroxylation of the fibre in ethanolic KOH solution. Fig. 7b also demonstrates the effect of the growth of the imprinted TiO_2 film on the surface of the U-shaped fibre. After 12.5 h of deposition, the growth of the film started to decrease the power transmission of light through the fibre until the transmission was nearly null (after 41 h of deposition the

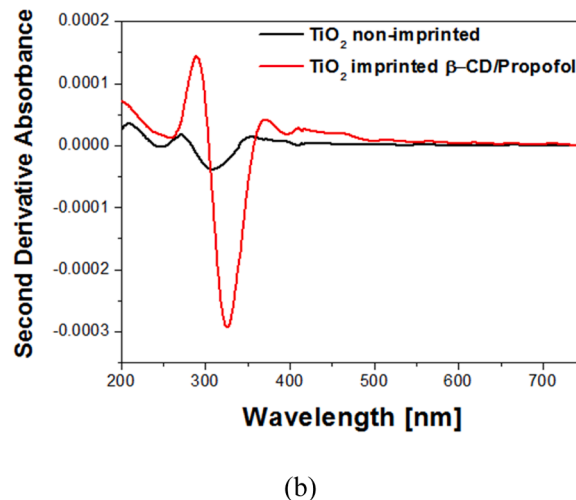


Fig. 6. (a) Comparison of the absorbance from imprinted and non-imprinted TiO_2 film deposited by LPD onto glass substrates. (b) Second derivative method from results shown in plot (a) following method of reference [30] by calculating first derivative of the spectrum, smoothing with a filter Savitzky-Golay (150 points and polynomial order 5), second derivative and filtering again with same parameters.

Table 1
Summary of the U-shaped probes used in this research.

U-shaped tested (RI sensitivity)	U-bend radius (mm)	LPD process	Deposition time
U1 (201.14 counts / 0.01 RI)	0.85	Concentrations from Set 1	ca. 41 h
U2 (234.97 counts / 0.01 RI)	0.71	Concentrations from Set 1	ca. 21 h
U3 (149.94 counts / 0.01 RI)	0.73	Concentrations from Set 1	ca. 18 h
U4 (168.21 counts / 0.01 RI)	0.82	Concentrations from Set 2	ca. 12 h
U5 (274.83 counts / 0.01 RI)	0.68	Concentrations from Set 2	ca. 12 h
U6 (190.68 counts / 0.01 RI)	0.72	Concentrations 25 mM:50 mM ([NH ₄) ₂ TiF ₆ :H ₃ BO ₃) without β - CD:Propofol	ca. 20 h

intensity decreased more than 90%).

After removal of the analyte propofol by immersing the U-shaped fibres in EtOH for 5 min, U2 and U3 from Table 1 were initially tested to demonstrate the binding of propofol on the U-shaped sensors (millimolar range and using the set-up shown in Fig. 3b). The sensor U2 was re-used after piranha solution (H₂SO₄: H₂O₂ = 3:1) cleaning, its sensitivity to RI was measured again to be reduced to 115.71 counts / 0.01 RI (234.97 counts / 0.01 RI), U2 was functionalized through the LPD process for 20 h and tested again for propofol binding (Fig. 8b). In Fig. 8a, the transmission spectra of U2 were recorded after different concentrations of propofol were continuously added dropwise in water (under stirring) using precision micro-pipettes. Fig. 8b compares the response of U2, the second use of U2 after cleaning/re-functionalization and the response from U3. The absolute change in light intensity (counts, vertical axis of Fig. 8b) was calculated from the intensity at maximum peak (663 nm) when the U-shaped sensors were immersed only in deionised water (concentration C0 in Fig. 8a) and measuring the absolute intensity change after adding different concentrations dropwise as shown in Fig. 8a and beyond the eight first concentrations. Section 4 of Supplementary Material provides dynamic measurements of U2 - U5 (from Fig. S10 to S13) when the change in the light intensity was

programmed to be recorded at 600 nm and every 5 ms.

Fig. 8b demonstrates the binding of propofol on the U-shaped sensors and showing a Langmuir type adsorption. The equilibrium binding constants in the millimolar range (185.18 (mM)⁻¹ and 99.50 (mM)⁻¹) were calculated as in reference [46] and they depend mainly on the sensitivity provided from the U-bend radii manufactured and the amount of time used for functionalization using the LPD process.

To demonstrate the effect of the sets of concentrations, deposition times (Table 1) during sensor functionalization (LPD process) and the difference between the imprinted and non-imprinted TiO₂ film for the measurement of propofol, Fig. 9 compares the response of U2 and two other U-shaped fibres (U4 and U5, Table 1) both having a similar sensitivity to refractive index change, functionalized with the same set of concentrations, and coated with the same deposition time. In addition, the response from a non-imprinted TiO₂ coated U-shaped fibre (U6, Table 1) was compared with the imprinted cases. All the responses plotted in Fig. 9 (micromolar range) were obtained using the set-up shown in Fig. 3b. The cases of U4, U5 and U6 used a stock propofol solution of 20 μ M and an initial volume of deionised water of 4 ml. Similarly, the absolute change in light intensity was measured at $\lambda = 663$ nm (maximum peak of spectra) with respect to the light intensity originally measured in deionised water. The lowest detected concentration using U2 was 1.0 μ M in the millimolar range (initial volume 20 ml and stock solution of 0.5 mM propofol) and lowest detected concentration of propofol using U4 and U5 was 0.69 μ M in the micromolar range (initial volume 4 ml and stock solution of 20 μ M propofol).

4. Discussion

The significant changes for the proton B in propofol and H3 and H5 for the host molecule (β - CD) in Fig. 4 are indicative of the inclusion occurrence of the aromatic side of propofol is mostly set inside the cavity of the host β - CD for any of the three concentrations tested in NMR spectroscopy, demonstrating the inclusion configuration between these host-guest molecules (Fig. 4b). The results presented in Section 3.1 and Supplementary Material have demonstrated the complexation between β - CD and propofol and the mechanism of this inclusion mechanism is mainly due to electrostatic forces and hydrophobic interactions [47]. Results of Fig. 4 indicate that the 1:1 ratio of β - CD and propofol are adequate to make a host-guest complexation, however, higher CD ratios can introduce a stronger equilibrium and protons A and C of propofol can be more shifted. The multiple hydroxy groups of β - CD react with

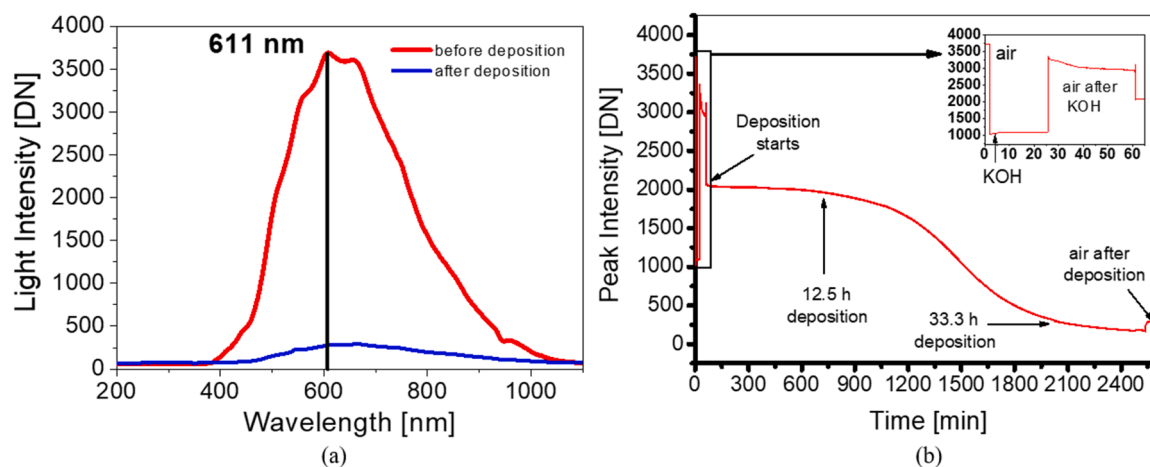


Fig. 7. (a) Transmission light spectra in counts (DN=Digital Number) recorded in air before and after deposition of the film for 41 h, using the set-up of Fig. 3b and U1 from Table 1. (b) Tracking of the single wavelength 611 nm before, during and after the film deposition for 41 h (the counts for the specific wavelength of 611 nm were recorded with an integration time of 5 ms). Laboratory room temperature and humidity were stable during all the experiment process (24 °C \pm 2 °C and 58%RH \pm 4%RH, respectively).

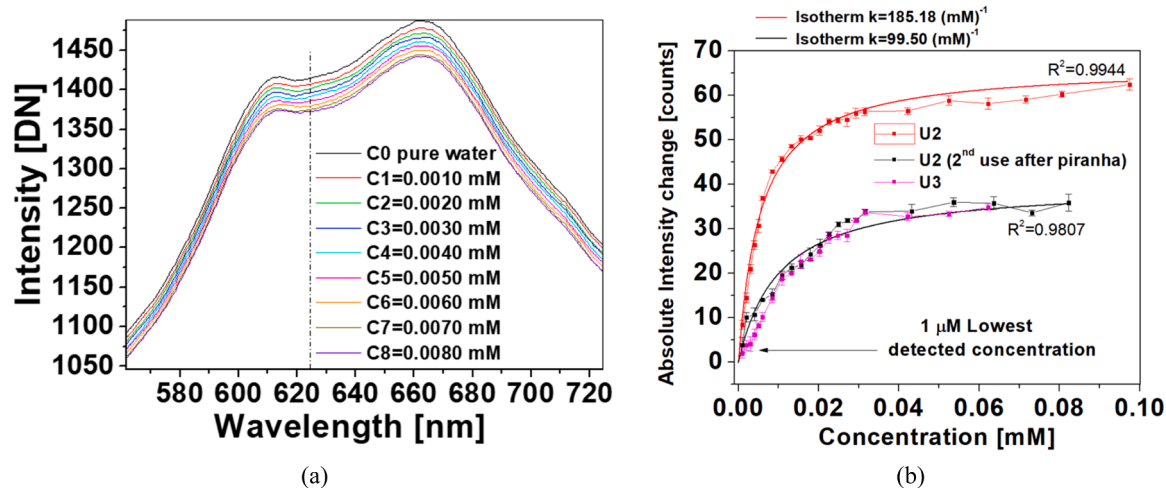


Fig. 8. (a) Change of the transmission spectrum in the coated sensor U2 (Table 1) after continuously adding dropwise the first eight concentrations of propofol (using a stock solution of 0.5 mM and an initial volume of 20 ml of deionised water). (b) U2 and U3 showed different sensitivities as Langmuir adsorption isotherms for the binding of propofol (all the error bars were measured as the standard deviation of the signal at 663 nm measured from three spectra at each concentration and a time between 3 and 5 min was allowed for stabilization of each concentration dropped in water).

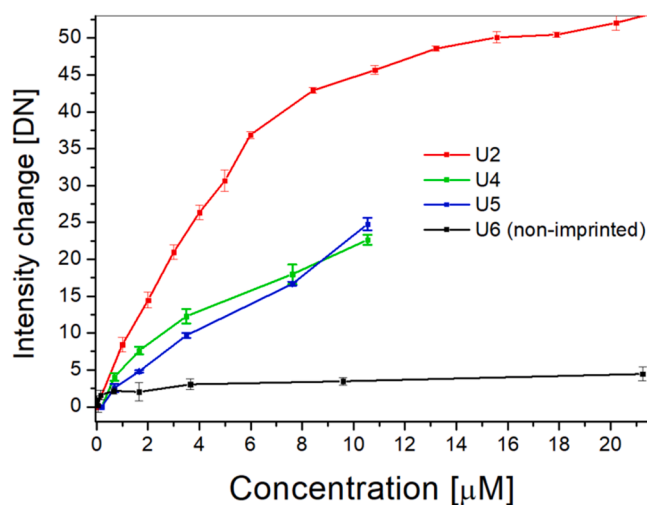


Fig. 9. Comparison of sensitivities for the low concentration range between U-shaped fibres coated with two different sets of concentrations (Table 1) and a non-imprinted TiO₂ coated fibre. All the error bars were measured as the standard deviation of the signal at 663 nm measured from three spectra at each concentration and a time between 3 and 5 min was allowed for stabilization of each concentration dropwise added to water.

the [Ti(OH)₆]²⁻ species generated by the hydrolysis reaction of [TiF₆]²⁻ (Supplementary Material) and previous studies [35] have demonstrated that mainly the hydroxy groups of the primary face of β-CD are the most active in a manner that the Ti species adsorb onto these hydroxy groups by hydrogen bonding. Fig. 10 exemplifies how the supramolecular host-guest interaction can be translated onto the surface of TiO₂ deposited onto the surface of OFS [48]. As explained in Section 2.3, the sensing mechanism via the host-guest interaction between β-CD and propofol produces a change in the effective refractive index of the coated U-shaped section and a change in the transmission of light (bending loss)

through the bent area.¹

The transient response of the U-shaped sensor based on the host-guest interaction can be understood in terms of the kinetic analysis and the association between β-CD and propofol described via Langmuir adsorption isotherms (Fig. 8b). As similar with Chen et al. [49], assuming the intensity response of the sensor is proportional to the host-guest complex concentration, the transient response depends on the association/dissociation rate constants and the concentrations of both immobilized β-CD and the amount of propofol (refer to Fig. S17, section 7 of Supplementary Material).

Fig. 8b demonstrates the binding of propofol on the U-shaped sensors follows a Langmuir type adsorption with different binding constants for every sensor tested in the millimolar range. In this concentration range, the sensors can be calibrated following the same procedure as reported in our previous research work [46], i.e., linearization of the experimental data can be obtained via the implementation of a reciprocal Langmuir isotherm to find the best linear fit and calculate the equilibrium binding constants.

ATR-FTIR and UV-Vis demonstrated spectroscopic differences between imprinted and non-imprinted TiO₂ films and the feasibility to imprint the proposed hybrid complex (Fig. 10) during the LPD process deployed in this research. Fig. 5 evidenced that the characteristic bending vibrations section (1400 – 1750 cm⁻¹) of pure TiO₂ is masked by hydroxyl groups from the organic complex of the imprinted TiO₂ film and the conformation of TiO₂ with the organic complex is evidenced through the appearance of the stretching modes in the 1110 – 1160 cm⁻¹ range. Similarly, the critical points (maximum and minimum in Fig. 6b) appearing at c.a. 286 nm and 325 nm evidenced the presence of β-CD and propofol in the imprinted TiO₂ film when compared to the non-imprinted case. Bailey et al. [41] have reported the wavelength 286 nm as attributable to the absorbance of propofol; Karim and Adnan [43], Kitamura and Imayoshi [44] and Özdemir and Biçer [36] have reported 260 nm as the maximum absorbance of β-CD. Nevertheless, the spectroscopic properties of the host-guest molecules tend to be modified as a result of the inclusion, usually to values higher than 300 nm for guest molecules already hosted by β-CD [29,36,43,44] and

¹ Refer to section 6 of Supplementary Material to verify that the presence of propofol does not affect the absorption of the film in the presence of the molecule in the wavelength range where the U-shaped sensor works. This was demonstrated via transmission spectroscopy (Fig. S16) in the working wavelength range demonstrated in this research.

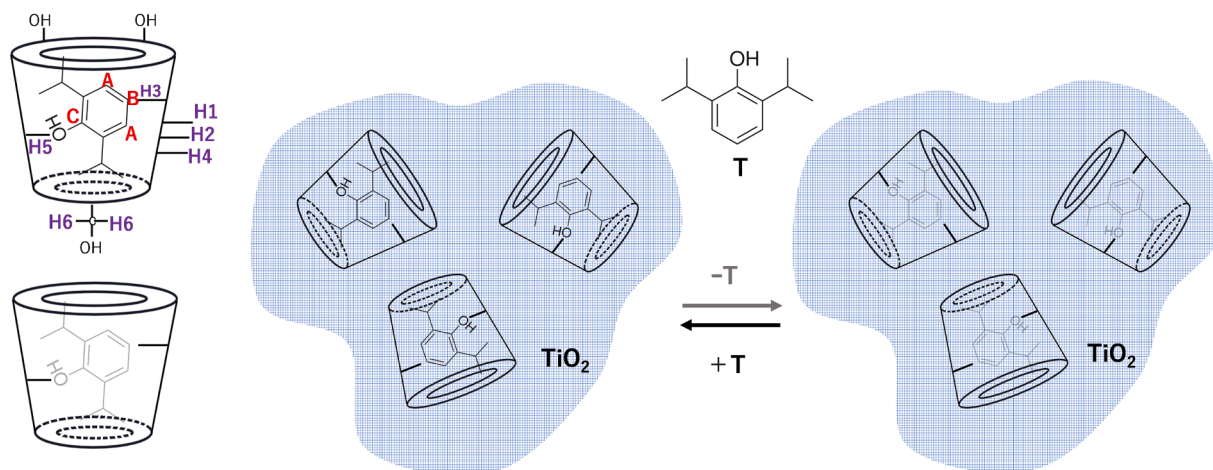


Fig. 10. Schematic of the hybrid film consisted of β -CD assisted propofol (template T) imprinting onto TiO_2 films. The Ti species are mainly adsorbed onto the hydroxy groups of C6 all around the β -CD molecule during hydrolysis and β -CD can self-assemble into regular composites and coordinate with Ti^{4+} ions (the initial nucleus for crystalline TiO_2) to form assemblies driven by intermolecular and Van der Waals forces [35,47,48].

this is clearly visible in the imprinted TiO_2 spectrum of Fig. 6.

The results shown in Fig. 8b evidence that the bend ratio (bending radius / core radius) impacts the sensitivity to refractive index. U2 outperformed U3 in detection at the millimolar range due to two factors: Smaller radius (original sensitivity to refractive index change) and longer deposition time (a major number of imprinted sites for binding) using the same set of deposition concentrations (Set 1 in Table 1).

The six U-shaped fibres fabricated in this research had a bend ratio of {8.5, 7.1, 7.3, 8.2, 6.8, 7.2} respectively. None of the cases fabricated in this research generated a bend ratio < 5 and simulations of Danny et al. [27] indicate that the RI sensitivity is similar in the range between 5 and 9 ratio but sensitivity increases largely when the bend ratio lies between 1.4 and 2.1 (considering bend-induced RI inhomogeneity) [27].

The sets of concentrations based on $[\text{NH}_4]_2\text{TiF}_6$: H_3BO_3 also had an impact on propofol detection. Despite that U4 and U5 were only tested in the micromolar range, the Set 2 of concentrations (50 mM: 100 mM) applied in U4 and U5 allowed to detect a concentration of 0.69 μM and better sensitivity for binding propofol than U3 coated with the Set 1 (25 mM: 50 mM). In addition, the growth of the imprinted film onto the U-shaped surface area was faster when using the Set 2 (12 h in average, data not shown here) than implementing with Set 1 (21 h, data not shown here). Sensitivity of the U-shaped sensor U2 was diminished after piranha cleaning, demonstrating that re-use of the same optical fibre sensor remains a challenge for future work, i.e., an ideal removal of TiO_2 coating using piranha solution needs to be further investigated to produce reproducible sensitivity. Similarly, in Supplementary Material (Fig. S18 of section 7), the sensor U2 was used two times consecutively to test reversibility of the sensor with a single wash of ethanol in between the measurements of propofol. The non-imprinted U-shaped sensor (U6) did not show significant response to the binding of propofol in both millimolar and micromolar range.

It is worth noting that changes in temperature and bulk refractive index will affect the response of the sensor and these need to be compensated for quantitative measurements to be achieved in practice. In the experiments shown in this paper, the effect of temperature on the sensitivity and linearity of the sensors tested in this research was not investigated in detail during the measurements of propofol presented in Section 3.4 (using the set-up of Fig. 3b), however, the temperature of the water solution was regularly monitored to be between 35 $^\circ\text{C}$ and 37 $^\circ\text{C}$ with laboratory thermometer. In practice, changes in refractive index and temperature can be compensated with the addition of one or more reference fibre probes [50,51]. Calibration curves (such as Fig. 9) of the sensors will be obtained for different concentrations of propofol and different refractive indices. We are currently exploring extending this

approach to breath measurements in the gas phase in which calibration at different refractive indices can be avoided.

5. Conclusions

The LPD process was used to functionalize U-shaped sensors with imprinted TiO_2 films for the measurement of propofol. A deposition time between 21 and 26 h was implemented to demonstrate the spectroscopically differentiation between imprinted and non-imprinted TiO_2 films (FTIR and UV-Vis respectively). The growth of the imprinted TiO_2 film was corroborated in Fig. 7 onto U-shaped sensors and exceeding a deposition time of 30 h would normally produce a loss of sensitivity as the transmission spectrum will decrease to zero. Section 5 of Supplementary Material presents Scanning Electron Microscope (SEM, Figs. S14 – S15) images of the thin film deposited on the optical fibre surface. According to the results shown in Figs. 8 and 9, the lowest detected concentration in aqueous solutions was 0.69 μM with the aid of β -CD as host compound for propofol measurement. A lack of detection was also demonstrated when a non-imprinted U-shaped sensor (Fig. 9) was tested under the same experimental conditions. This supports the selectivity of the sensor due to the presence of the host-guest molecules (β -CD and propofol) during the molecular imprinting process via the LPD technique (Section 1 of Supplementary Material). Baggiani et al. [52] have reported the connection between the binding characteristics of imprinted and non-imprinted polymers and they have supported that the nature of the binding properties of the resulting imprinted materials are determined by three main factors: composition of the prepolymerization mixture (set of concentrations), experimental conditions (temperature), and the type of polymerization or imprinting mechanism used.

The approaches presented in the literature review have attempted to provide an on-line and more compact device for measuring propofol concentrations in aqueous or blood samples. Most of these approaches managed to perform rapid detection of propofol (ca. 5 min) within the expected clinical range in blood samples: 0.1 $\mu\text{g}/\text{ml}$ – 10 $\mu\text{g}/\text{ml}$. The application of propofol measurement using optical fibre technology still needs engineering improvements for its clinical application. As comparison, some approaches (e.g., [6], $\text{LoD} = 1.4 \mu\text{M} = 0.25 \mu\text{g}/\text{ml}$) are expensive to fabricate. Others (e.g. [9], $\text{LoD} = 0.65 \mu\text{g}/\text{ml}$) need to use additional reagents to apply a colorimetry approach based on absorbance or use expensive optical filters and collimators [10], or use non-specific method of extraction such as SPE (e.g. [12], $\text{LoD} = 0.75 \mu\text{g}/\text{ml}$). In contrast, the U-shaped measurement proposed in this research detected down to a concentration of 0.69 μM (0.12 $\mu\text{g}/\text{ml}$) in

aqueous solution and the biosensor proposed offers an alternative and less expensive option of detection since interrogation of U-shaped fibres only requires a single LED and a photodetector. Moreover, optical fibre sensors can be integrated easily on indwelling catheters to facilitate in situ measurement. Future work still needs to improve the statistical detection limit and selectivity to target propofol needs to be tested in whole blood samples or lysed blood samples. Similarly, future work will investigate: (1) cross-sensitivity towards interfering compounds such as those studied in reference [12]; (2) verification on whether the imprinted TiO₂ film supports lossy resonance modes to increase coupling, evanescent field enhancement and the increase of sensitivity for the measurement of propofol or similar compounds; and (3) the compensation in the effect of temperature and refractive index on the sensor response via including a reference probe to perform measurements in-situ.

CRedit authorship contribution statement

Francisco U. Hernandez: Conceptualisation, Methodology, Software, Validation, Formal analysis, Investigation, Project management, Writing - original draft. **T. Wang:** Formal analysis, Investigation. **Seung-Woo Lee:** Conceptualisation, Methodology, Validation, Writing - review & editing, Supervision, Project administration, Funding acquisition. **A. Norris:** Validation, Investigation, Writing- review & editing. **Liang-Liang Liu:** Formal analysis, Investigation. **B.R. Hayes-Gill:** Methodology, Writing - review & editing, Supervision, Project administration. **S.P. Morgan:** Conceptualisation, Methodology, Writing - review & editing, Supervision, Project administration, Funding acquisition. **Serhiy Korposh:** Conceptualisation, Methodology, Writing - review & editing, Supervision, Project administration, Funding acquisition.

Declaration of Competing Interest

The authors declare that they have no known competing financial interests or personal relationships that could have appeared to influence the work reported in this paper.

Data availability

Data will be made available on request.

Acknowledgments

We would like to thank The Engineering and Physical Sciences Research Council UK (EPSRC, Grant Number EP/N026985/1) and the National Council of Science and Technology of Mexico (CONACyT). We would also like to thank the Nanoscale and Microscale Research Centre (nmRC) at the University of Nottingham for providing access to the instrumentation and PhD student Jesus Molinar Diaz for the technical support provided at the nmRC. Thanks to Dr. Chengyang He from the Optics and Photonics group for useful suggestions during the paper preparation.

Appendix A. Supporting information

Supplementary data associated with this article can be found in the online version at [doi:10.1016/j.snb.2022.132653](https://doi.org/10.1016/j.snb.2022.132653).

References

- [1] A. Lim, S. Braat, J. Hiller, B. Riedel, Inhalational versus propofol-based total intravenous anaesthesia: practice patterns and perspectives among Australasian anaesthetists, *Anaesth. Intensive Care* 46 (5) (2018) 480–487.
- [2] W.-K. Lee, M.-S. Kim, S.-W. Kang, S. Kim, J.-R. Lee, Type of anaesthesia and patient quality of recovery: a randomized trial comparing propofol-remifentanyl total i.v. anaesthesia with desflurane anaesthesia, *Br. J. Anaesth.* 114 (4) (2015) 663–668.
- [3] F. McGain, J. Muret, C. Lawson, J. Sherman, Environmental sustainability in anaesthesia and critical care, *Br. J. Anaesth.* 125 (5) (2020) 680–692.
- [4] A. Nimmo, A. Absalom, O. Bagshaw, A. Biswas, T. Cook, A. Costello, S. Grimes, D. Mulvey, S. Shinde, T. Whitehouse, M. Wiles, Guidelines for the safe practice of total intravenous anaesthesia (TIVA): Joint Guidelines from the Association of Anaesthetists and the Society for Intravenous Anaesthesia, *Anaesthesia* 74 (2) (2019) 211–224.
- [5] Z. Al-Rifai, D. Mulvey, Principles of total intravenous anaesthesia: practical aspects of using total intravenous anaesthesia, *BJA Educ.* 16 (8) (2016) 276–280.
- [6] C.-C. Hong, P.-H. Chang, C.-C. Lin, C.-L. Hong, A disposable microfluidic biochip with on-chip molecularly imprinted biosensors for optical detection of anesthetic propofol, *Biosens. Bioelectron.* 25 (2010) 2058–2064.
- [7] A. Takita, K. Masui, T. Kazama, On-line monitoring of end-tidal propofol concentration in anesthetized patients, *Anesthesiology* 106 (2007) 659–664.
- [8] M. Grossherr, A. Hengstenberg, T. Meier, L. Dibbelt, B.W. Igl, A. Ziegler, P. Schmucker, H. Gehring, Propofol concentration in exhaled air and arterial plasma in mechanically ventilated patients undergoing cardiac surgery, *Br. J. Anaesth.* 102 (5) (2009) 608–613.
- [9] L. Li, Y. Li, Study of az-coupling derivatization by sequential injection coupled with spectrophotometric optical fibre detection for propofol analysis, *Anal. Methods* 8 (2016) 6176–6184.
- [10] L. Li, H. Ding, B. Di, W. Li, J. Chen, Rapid detection of propofol in whole blood using an automated on-line molecularly imprinted pretreatment coupled with optical fibre detection, *Analyst* 137 (2012) 5632–5638.
- [11] L. McLaughran, L.J. Voss, R. Oliver, M. Petcu, P. Schaare, J.P. Barnard, J. W. Sleight, Rapid measurement of blood propofol levels: A proof of concept study, *J. Clin. Monit. Comput.* 20 (2006) 109–115.
- [12] B. Liu, D.M. Pettigrew, S. Bates, P.G. Laitenberger, G. Troughton, Performance evaluation of a whole blood propofol analyser, *J. Clin. Monit. Comput.* 26 (2012) 29–36.
- [13] F. Kivlehan, E. Chaum, E. Lindner, Propofol detection and quantification in human blood: the promise of feedback controlled, closed-loop anesthesia, *Analyst* 140 (2015) 98–106.
- [14] F. Stradolini, A. Tuoheti, T. Kilic, D. Demarchi, S. Carrara, Raspberry-Pi based system for propofol monitoring, *Integration* 63 (2018) 213–219.
- [15] F.U. Hernandez, T. Wang, S.-W. Lee, A. Norris, S.P. Morgan, R. Correia, B.R. Hayes-Gill, S. Korposh, Propofol detection using optical fibre long period grating sensors with molecularly imprinted host-guest binding sites in TiO₂ films, 26th Int. Conf. Opt. Fiber Sens. (2018) TuE72.
- [16] R. Correia, S. James, S.-W. Lee, S.P. Morgan, S. Korposh, Biomedical application of optical fibre sensors, *J. Opt.* 20 (2018), 073003.
- [17] R.T. Ghahrizjani, H. Sadeghi, A. Mazaheri, A. Novel, Method for onLine monitoring engine oil quality based on tapered optical fiber sensor, *IEEE Sens. J.* 16 (10) (2016) 3551–3555.
- [18] T. Irie, K. Uekama, Cyclodextrins in peptide and protein delivery, *Adv. Drug Deliv. Rev.* 36 (1) (1999) 101–123.
- [19] B. Voncina, V. Vivod, Cyclodextrins in Textile Finishing, in: M. Günay (Eds.), Eco-Friendly Textile Dyeing and Finishing, *Intech Open*, 2013, pp. 53–75.
- [20] V. Caligr, Cyclodextrins, *BioFiles* 3 (3) (2008) 32–33.
- [21] F. Maestrelli, M. Bragagni, P. Mura, Advanced formulations for improving therapies with anti-inflammatory or anaesthetic drugs: A review, *J. Drug Deliv. Sci. Technol.* 32 (2016) 192–205.
- [22] A. Ejchart, W. Kozminski, NMR of Cyclodextrins and Their Complexes, in: H. Dodziuk (Eds.), *Cyclodextrins and Their Complexes*, Wiley-VCH Verlag GmbH & Co. KGaA., Weinheim, 2006, pp. 231–254.
- [23] S.K. Khijwania, K.L. Srinivasan, J.P. Singh, An evanescent-wave optical fiber relative humidity sensor with enhanced sensitivity, *Sens. Actuators B Chem.* 104 (2005) 217–222.
- [24] R.T. Schermer, J.H. Cole, Improved bend loss formula verified for optical fiber by simulation and experiment, *IEEE J. Quantum Electron* 43 (10) (2007) 899–909.
- [25] N. Paliwal, N. Punjabi, J. John, S. Mukherji, Design and Fabrication of Lossy Mode Resonance Based U-Shaped Fiber Optic Refractometer Utilizing Dual Sensing Phenomenon, *J. Light. Technol.* 34 (17) (2016) 4186–4193.
- [26] D. Kaur, V.K. Sharma, A. Kapoor, High sensitivity lossy mode resonance sensors, *Sens. Actuators B Chem.* 198 (2014) 366–376.
- [27] C.G. Danny, M.D. Raj, V.V. Sai, Investigating the refractive index sensitivity of u-bent fiber optic sensors using ray optics, *J. Light. Technol.* 38 (6) (2020) 1580–1588.
- [28] Z. Tang, D. Gomez, C. He, S. Korposh, S.P. Morgan, R. Correia, B. Hayes-Gill, K. Setchfield, L. Liu, A U-shape fibre-optic pH sensor based on hydrogen bonding of ethyl cellulose with a sol-gel matrix, *J. Light. Technol.* 39 (5) (2021) 1557–1564.
- [29] G. Granero, C. Garnero, M. Longhi, Second derivative spectrophotometric determination of trimethoprim and sulfamethoxazole in the presence of hydroxypropyl-β-cyclodextrin (HP-β-CD), *J. Pharm. Biomed. Anal.* 29 (2002) 51–59.
- [30] S. Kus, Z. Marczenko, N. Obarski, Derivative UV–VIS spectrophotometry in analytical chemistry, *Chem. Anal. (Wars.)* 41 (1996) 899–927.
- [31] G.N. Reiner, L. Fernandes Fraceto, E. de Paul, M.A. Perillo, D.A. García, Effects of gabaergic phenols on phospholipid bilayers as evaluated by ¹H NMR, *J. Biomater. Nanobiotechnol.* 4 (2013) 28–34.
- [32] E. Locci, S. Lai, A. Piras, B. Marongiu, A. Lai, 13C-CPMAS and ¹H NMR study of the inclusion complexes of ss-cyclodextrin with carvacrol, thymol, and eugenol prepared in supercritical carbon dioxide, *Chem. Biodivers.* 1 (2004) 1354–1366.
- [33] National Institute of Standards and Technology. U.S. Department of Commerce, 2,6-Diisopropylphenol, (<http://webbook.nist.gov/cgi/cbook.cgi?ID=C2078548&Mask=80>). (Accessed 5 July 2017).

- [34] Y. Jia-Guo, Y. Huo-Gen, C. Bei, Z. Xiu-Jian, Y. Jimmy C, H. Wing-Kei, The effect of calcination temperature on the surface microstructure and photocatalytic activity of TiO₂ thin films prepared by liquid phase deposition, *J. Phys. Chem. B* 107 (2003) 13871–13879.
- [35] S.H. Toma, J.A. Bonacin, K. Araki, H.E. Toma, Selective host-guest interactions on mesoporous TiO₂ films modified with carboxymethyl- β -cyclodextrin, *Surf. Sci.* 600 (2006) 4591–4597.
- [36] N. Özdemir, E. Biçer, Voltametric, spectroscopic and thermal studies on the binding of some heterocyclic azo compounds with α - and β -cyclodextrins: ph effect and association affinity, *Russ. J. Electrochem.* 53 (5) (2017) 486–499.
- [37] J. Feng, A. Miedaner, P. Ahrenkiel, M.E. Himmel, C. Curtis, D. Ginley, Self-Assembly of Photoactive TiO₂-Cyclodextrin Wires, *J. Am. Chem. Soc. Commun.* 127 (2005) 14968–14969.
- [38] J.C. Yu, Z.-T. Jiang, H.-Y. Liu, J. Yu, L. Zhang, β -Cyclodextrin epichlorohydrin copolymer as a solid-phase extraction adsorbent for aromatic compounds in water samples, *Anal. Chim. Acta* 477 (2003) 93–101.
- [39] Z. Zheng, L. Zhang, Y. Liu, H. Wang, A facile and novel modification method of β -cyclodextrin and its application in intumescent flame-retarding polypropylene with melamine phosphate and expandable graphite, *J. Polym. Res* 4 (2016) 74–91.
- [40] D. Zhao, L. Zhao, C.-S. Zhu, Water-insoluble β -cyclodextrin polymer crosslinked by citric acid: synthesis and adsorption properties toward phenol and methylene blue, *J. Incl. Phenom. Macrocycl. Chem.* 63 (2009) 195–201.
- [41] L.C. Bailey, K.T. Tang, B.A. Rogozinski, The determination of 2,6-diisopropylphenol (propofol) in an oil in water emulsion dosage form by high-performance liquid chromatography and by second derivative UV spectroscopy, *J. Pharm. Biomed. Anal.* 9 (6) (1991) 501–506.
- [42] C. Balestrieri, G. Colonna, A. Giovane, G. Irace, L. Servillo, Second-derivative spectroscopy of proteins, *Eur. J. Biochem.* 90 (1978) 433–440.
- [43] Z. Karim, R. Adnan, The β -cyclodextrin-chitosan inclusion complex: characterization and application in the removal of pesticides in wastewater, *Arch. Environ. Sci.* 6 (2012) 1–12.
- [44] K. Kitamura, N. Imayoshi, Second-derivative spectrophotometric determination of the binding constant between chlorpromazine and β -cyclodextrin in aqueous solutions, *Anal. Sci.* 8 (1992) 497–501.
- [45] S. Korposh, S.-W. Lee, S.W. James, R.P. Tatam, Refractive index sensitivity of fibre-optic long period gratings coated with SiO₂ nanoparticle mesoporous thin films, *Meas. Sci. Technol.* 22 (7) (2011) 10.
- [46] L. Marques, F.U. Hernandez, S.W. James, S.P. Morgan, M. Clark, R.P. Tatam, S. Korposh, Highly sensitive optical fibre long period gratings biosensor anchored with silica core gold shell nanoparticles, *Biosens. Bioelectron.* 75 (2016) 222–231.
- [47] S. Saha, A. Roy, K. Roy, M.N. Roy, Study to explore the mechanism to form inclusion complexes of β -cyclodextrin with vitamin molecules, *Nat. Sci. Rep.* 6 (2016) 35764.
- [48] L. Li, X. Sun, Y. Yang, N. Guan, F. Zhang, Synthesis of anatase TiO₂ nanoparticles with β -cyclodextrin as a supramolecular shell, *Chem. Asian J.* 1 (2006) 664–668.
- [49] L.H. Chen, C.C. Chan, K. Ni, P.B. Hu, T. Li, W.C. Wong, P. Balamurali, R. Menon, M. Shaillender, B. Neu, C.L. Poh, X.Y. Dong, X.M. Ang, P. Zu, Z.Q. Tou, K.C. Leong, Label-free fiber-optic interferometric immunosensors based on waist-enlarged fusion taper, *Sens. Actuators B Chem.* 178 (2013) 176–184.
- [50] A.Y. Tan, S.M. Ng, P.R. Stoddart, H.S. Chua, Trends and applications of U-shaped fiber optic sensors: a review, *IEEE Sens. J.* 21 (1) (2021) 120–131.
- [51] F. Chiavaioli, C.A.J. Gouveia, P.A.S. Jorge, F. Baldini, Towards a uniform metrological assessment of grating-based optical fiber sensors: from refractometers to Biosensors, *Biosensors* 7 (2) (2017) 23.
- [52] C. Baggiani, C. Giovannoli, L. Anfossi, C. Passini, P. Baravalle, G. Giraudi, A connection between the binding properties of imprinted and nonimprinted polymers: a change of perspective in molecular imprinting, *J. Am. Chem. Soc.* 134 (2012) 1513–1518.

Francisco U. Hernandez: Francisco Ulises Hernandez Ledezma is currently a researcher fellow in the University of Nottingham and MBA student at the Nottingham Business School (Nottingham Trent University). His research has involved the adaptation of optical fibre technology in different industry projects. His work as R&D engineer has generated publications involving the integration of optical fibre sensors with smart textiles for sports and healthcare applications. Similarly, his research has demonstrated novel approaches

for developing chemical sensors using optical fibre sensors and the integration of these sensors in medical equipment usually deployed in the intensive care unit of hospitals.

T. Wang: Dr. Tao Wang was born in Dalian, China, in 1986. He received B.S., M.S. and Ph. D. degrees in Chemical Engineering from the University of Kitakyushu, Japan, in 2012, 2014 and 2017, respectively. He worked at the University of Kitakyushu as a postdoctoral researcher and engineering advisor. From 2018–2019, he served as an engineer with Nihon Dempa Kogyo Co., Ltd, Japan. Since 2022, he is working at the Department of Materials Process Engineering, Nagoya University, as a project researcher. His research interests include chemical sensors for bio-medical applications.

Seung-Woo Lee: S-W Lee is a professor in the Faculty of Environmental Engineering at the University of Kitakyushu. He leads a group to combine nanomaterials with various transducers to develop chemical sensors for medical diagnosis, food quality assessment, environmental monitoring, etc. Recently, he has founded a new project for medical diagnosis based on the discovery of small molecule biomarkers, including volatile organic compounds (VOCs) coming from the human body and cells. He has also devoted a long time to surface chemistry related to thin films and self-assembly.

A. Norris: Andrew Norris, MB ChB University of Sheffield Medical School 1986. Current post consultant anesthesiologist and department chairman, anesthesiology, King Faisal Specialist Hospital and Research Centre, Riyadh, Saudi Arabia. Formerly, consultant anaesthetist Nottingham University Hospitals NHS Trust 1997–2019. Previously Honorary Associate Clinical Professor, University of Nottingham, Division of Neuroscience, Faculty of Health Sciences. Head of School, East Midlands School of Anaesthesia 2014–2017, Lead Regional Advisor, RCoA 2011–2012, Examiner RCoA 2007–2019, Programme Director Nottingham and East Midlands 2003–2007. In addition to postgraduate medical education, research interests include airway management and development and evaluation of optical technologies in healthcare.

B.R. Hayes-Gill: Barrie Hayes-Gill, FREng, is Professor of Medical Devices and Electronic Systems at the University of Nottingham. His research covers a broad range of the application of electronic engineering and optical systems to medical devices with an emphasis on technology transfer. Some of his recent work has involved the deployment of an optical sensor in a newborn's cap to monitor heart rate and oxygen saturation at birth along with the deployment of fibre optic sensors in wearable medical devices in both hospital and home settings. Most significantly he has developed a wearable fetal monitor for mothers at birth which is now being deployed in thousands of births around the world. He is a Fellow of The Royal Academy of Engineering, Chartered Engineer and Fellow of the Institution of Engineering Technology.

S. P. Morgan: Stephen Morgan is Professor of Biomedical Engineering at the University of Nottingham. His research involves the development of medical devices with sensing capability. For example, he is currently developing a novel endotracheal tube that can monitor the microcirculation at the cuff/trachea interface and a smart wound dressing for monitoring healing rate and infection. His work has involved close collaboration with industry partners such as Footfalls and Heartbeats (UK), P3 Medical, Surepulse Medical and Moor Instruments. He is a Royal Society Industry Fellow and Director of the Centre for Healthcare Technologies which aims to bring together key stakeholders, capabilities, and expertise to support the rapid translation of scientific discoveries into healthcare adoption.

S. Korposh: Serhiy Korposh received both his bachelor and master degrees in 2001 and 2002 respectively in physics from Uzhgorod National University, Transcarpathia (Ukraine) and Ph.D. degree from Cranfield University in 2007. He worked as a post-doctoral researcher on development of the novel materials for chemical sensors in the Graduate School of Environmental Engineering of the University of Kitakyushu from 2008 to 2012. From 2012–2013 he worked as a research fellow in the Department of Engineering Photonics, Cranfield University. Since 2022 he is Professor in Electronics, Nanoscale Bioelectronics and Biophotonics at the University of Nottingham. His research interest lies in the field of development of fibre-optic chemical sensors modified with the sensitive materials and their applications in healthcare and environmental monitoring.